APPLICATIONS OF A NEXT-GENERATION MDAC DISCRIMINATION PROCEDURE USING TWO-DIMENSIONAL GRIDS OF REGIONAL P/S SPECTRAL RATIOS

Mark D. Fisk[1], Steven R. Taylor[2], Howard J. Patton[3], and William R. Walter[4]

Alliant Techsystems[1], Rocky Mountain Geophysics, LLC[2], Los Alamos National Laboratory[3], and Lawrence Livermore National Laboratory[4]

Sponsored by National Nuclear Security Administration

Contract No. DE-AC52-07NA28116
Proposal No. BAA07-46

ABSTRACT

Using extensions of theoretical source models for earthquakes and explosions, Fisk (2006, 2007) provided a consistent model-based explanation of the frequency dependence of regional P/S discriminants at all major nuclear test sites as mainly due to larger systematic differences in P- and S-wave corner frequencies for explosions than earthquakes, as well as different spectral shapes. This project focuses on exploiting this new understanding to improve discrimination of earthquakes and explosions using regional data. The main objective is to develop and test an innovative processing and discrimination procedure, based on robust features of multi-dimensional spectral ratios for regional seismic phases, and using comparisons to source models. In this paper, two-dimensional grids of P/S spectral ratios for all combinations of frequencies of P- and S-wave spectra are shown to exhibit much greater differences in relative spectral amplitudes and shapes between explosions and earthquakes than considered before. The approach builds naturally upon the Magnitude and Distance Amplitude Correction (MDAC) technique (Taylor and Hartse, 1998; Taylor et al., 2002; Walter and Taylor, 2002), correcting the spectra for source, geometrical spreading, attenuation, and site effects. The analysis is first applied to underground nuclear explosions (UNEs) at the Semipalatinsk Test Site and regional earthquakes recorded by station WMQ (Urumchi, China). Measurements from the grids are considered that include a traditional Pn/Lg discriminant, a broadband cross-spectral ratio (high-frequency Pn and low-frequency Lg), and the root-mean-squared misfit to the MDAC model, under the hypothesis of a Brune (1970) earthquake source. The latter two, especially cross-spectral Pn/Lg, are shown to vastly improve discrimination performance over traditional Pn/Lg and to increase the applicability rate due to higher Lg signal-to-noise at lower frequencies. Similar analyses and improvements in discrimination performance are shown for UNEs at the Lop Nor Test Site in China and nearby earthquakes that were recorded by up to 19 regional seismic stations. Improvements are also demonstrated for earthquakes and UNEs at the Nevada Test Site (NTS), although geological differences between the test sites – mainly gas porosity of emplacement media – prompt the use of Lg spectral amplitudes at higher frequencies for NTS. Comparisons to source models may be used to confirm the physical basis of the discrimination results. The performance of various discriminants at test sites with different geology are discussed in the context of the theoretical source models.

Report Documentation Page

Form Approved
OMB No. 0704-0188

1. REPORT DATE	2. REPORT TYPE	3. DATES COVERED
SEP 2008		**00-00-2008 to 00-00-2008**

4. TITLE AND SUBTITLE	5a. CONTRACT NUMBER
Applications of a Next-Generation MDAC Discrimination Procedure Using Two-Dimensional Grids of regional P/S Spectral Ratios	5b. GRANT NUMBER
	5c. PROGRAM ELEMENT NUMBER
6. AUTHOR(S)	5d. PROJECT NUMBER
	5e. TASK NUMBER
	5f. WORK UNIT NUMBER
7. PERFORMING ORGANIZATION NAME(S) AND ADDRESS(ES) **Lawrence Livermore National Laboratory,PO Box 808,Livermore,CA,94551-0808**	8. PERFORMING ORGANIZATION REPORT NUMBER
9. SPONSORING/MONITORING AGENCY NAME(S) AND ADDRESS(ES)	10. SPONSOR/MONITOR'S ACRONYM(S)
	11. SPONSOR/MONITOR'S REPORT NUMBER(S)

12. DISTRIBUTION/AVAILABILITY STATEMENT
Approved for public release; distribution unlimited

13. SUPPLEMENTARY NOTES
Proceedings of the 30th Monitoring Research Review: Ground-Based Nuclear Explosion Monitoring Technologies, 23-25 Sep 2008, Portsmouth, VA sponsored by the National Nuclear Security Administration (NNSA) and the Air Force Research Laboratory (AFRL)

14. ABSTRACT
see report

15. SUBJECT TERMS

16. SECURITY CLASSIFICATION OF:			17. LIMITATION OF ABSTRACT	18. NUMBER OF PAGES	19a. NAME OF RESPONSIBLE PERSON
a. REPORT	b. ABSTRACT	c. THIS PAGE			
unclassified	**unclassified**	**unclassified**	**Same as Report (SAR)**	**10**	

OBJECTIVES

The main objective is to develop and test an enhanced discrimination procedure, based on robust characteristics of multi-dimensional spectral ratios for regional seismic phases. The approach builds naturally upon the existing MDAC procedure by exploiting differences of relative spectral amplitudes and shapes due to source type that are currently not used, but are visually apparent. Another objective is to provide direct comparison of the empirical discrimination results to model calculations to confirm the physical basis and, in turn, to better understand source mechanisms that affect regional discriminants. Key tasks are to (1) compute 2D spectral ratios (Pn/Sn, Pn/Lg, Lg/Lg, etc.) for earthquakes and explosions at nuclear test sites, using spectra corrected for source, distance, and site effects; (2) compare the empirical spectra to theoretical predictions based on modified Brune (1970) and Mueller and Murphy (1971) [MM71] source models for P and S waves generated by earthquakes and explosions, respectively; (3) evaluate distinctive features of the 2D spectral ratios that capture model-based spectral differences of the event types and enhance discrimination performance; (4) quantify uncertainties of the corrected spectra for various regions, stations, and event types, as well as misfits of empirical and model 2D spectral ratio comparisons; (5) develop a robust discrimination procedure and evaluate its performance on broad sets of data; and (6) develop visualization techniques that allow the discrimination results and model comparisons to be assessed by a human analyst.

RESEARCH ACCOMPLISHED

We have computed spectra of Pn, Pg, Sn, and/or Lg for explosions at the Semipalatinsk, Lop Nor, Novaya Zemlya, and Nevada Test Sites (STS, LNTS, NZTS, NTS, respectively) and regional earthquakes. We used phase-specific window lengths, with onsets prior to analyst picks of the regional phase arrivals to allow for a 10% cosine taper. We smoothed the log spectra using a moving 0.5 Hz window and corrected for instrument response. Using the MDAC approach, we then corrected the spectra for distance, site, and source terms, assuming a Brune (1970) earthquake source model. Details of the models and the parameters are provided by Fisk (2006, 2007) for the various test sites.

In the discrimination analysis below, we apply two hypothesis tests, based on the t-distribution, to assess whether an event is rejected as belonging to the explosion or earthquake populations. Let $\bar{R}$ denote station-averaged, MDAC-corrected log(Pn/Lg) in a given frequency band. An event is rejected as belonging to the explosion population if:

$$\frac{\bar{R} - \hat{\mu}_{R,\,EX}}{\sqrt{\dfrac{(N_{EX}-1)\hat{\sigma}^2_{R,\,EX} + (N_m - 1)\hat{\sigma}^2_m}{N_{EX}+N_m-2}\left(\dfrac{1}{N_{EX}} + \dfrac{1}{N_m}\right)}} < -t_\alpha(N_{EX}+N_m-2)\,, \qquad \text{(EQ 1)}$$

where $\hat{\mu}_{R,\,EX}$ and $\hat{\sigma}_{R,\,EX}$ are the mean and standard deviation of $\bar{R}$ estimated from N_{EX} explosions in the multi-station training set, and $\hat{\sigma}_m$ is the standard deviation of $\bar{R}$ estimated from N_m stations for the test event. Likewise, an event is rejected as belonging to the earthquake set if:

$$\frac{\bar{R} - \hat{\mu}_{R,\,EQ}}{\sqrt{\dfrac{(N_{EQ}-1)\hat{\sigma}^2_{R,\,EQ} + (N_m - 1)\hat{\sigma}^2_m}{N_{EQ}+N_m-2}\left(\dfrac{1}{N_{EQ}} + \dfrac{1}{N_m}\right)}} > t_\alpha(N_{EQ}+N_m-2)\,. \qquad \text{(EQ 2)}$$

In these expressions, $t_\alpha(N)$ is the (1–α)-percentile of the t-distribution with N degrees of freedom. In the following applications, the significance level is set at $\alpha = 0.005$, unless otherwise stated. Events rejected by one test and not by the other are categorized as the latter event type. Events rejected by both or not rejected by either are categorized as *undetermined*. Using two criteria allows separate control of the error rates and clear definition of *undetermined*.

Figure 1 depicts locations of earthquakes, UNEs at STS and LNTS, and most regional seismic stations. Many STS UNEs up to 1989 were recorded digitally by WMQ (Urumqi, China) and BRV (Borovoye, Kazakhstan). For STS, we use WMQ recordings, which are better quality than BRV data. We also processed 74 earthquakes during 1995 to 2002, ranging from mb 3.2 to 5.9, and recorded at regional distances by WMQ. We chose the events over a broad region because there was only one earthquake during this time period within 280 km of STS. Many of the events since mid 1994, including ten LNTS UNEs, were recorded digitally by up to 19 regional stations. For LNTS, we processed all available regional recordings for the UNEs and a sample of 43 earthquakes (mb 3.5 to 5.4) in the box that contains LNTS in Figure 1. Fisk (2006) provides further information regarding these data and examples of the spectra and model comparisons.

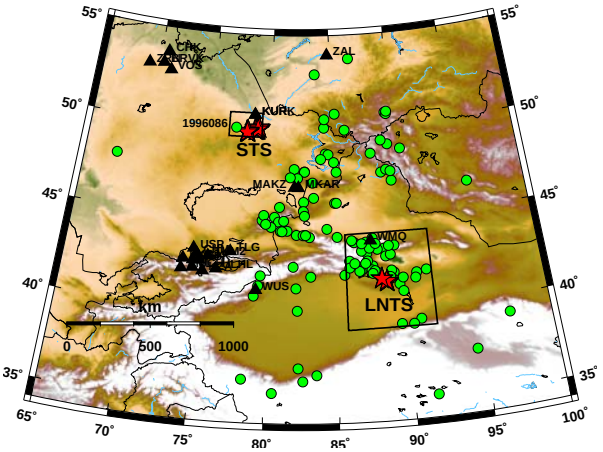

Figure 1. Locations of UNEs (stars), earthquakes (circles), and most of the digital seismic stations (triangles) within 2000 km of STS and LNTS.

Semipalatinsk Test Site

Figure 2 shows Pn/Lg spectral ratios, corrected for site and distance effects, for the Soviet Joint Verification Experiment (JVE), a small UNE at Degelen, and a nearby earthquake on 1996/03/26 using WMQ data only (cyan) and averaging over 17 stations (green). Figure 2 also shows the Brune model prediction (gray curve) for the earthquake and MM71 model results for each UNE (black curves). The models represent the empirical Pn/Lg spectral ratios quite well, and explain the frequency dependence of P/S discrimination performance as mainly due to larger differences in explosion P and S corner frequencies and stronger spectral shapes, including overshoot, for explosions. Fisk (2006) shows similar frequency dependence for Pn/Lg and/or Pn/Sn at the Lop Nor and Novaya Zemlya test sites.

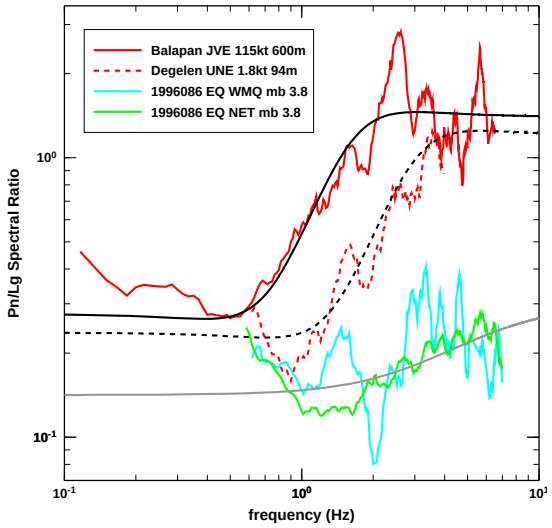

Figure 2. Empirical and model Pn/Lg spectral ratios using WMQ data for the JVE, a small UNE at Degelen, and for a nearby earthquake using WMQ data only and averaging over 17 regional stations.

Figure 2 not only illustrates a model-based explanation of why P/S discrimination performance is usually better at higher frequencies (i.e., near or above the Pn corner frequency for explosions, which depends on source size), but also that the earthquakes and explosions have different spectral shapes, that should be exploited to improve discrimination. To illustrate this, Figure 3 compares 2D empirical (left) and model (right) grids of Pn/Lg spectral ratios for the earthquake (top), the JVE at Balapan (middle), and a UNE at Degelen (bottom). The Pn and Lg spectra were corrected for Q, spreading, site effects, and a Brune source term (under the earthquake hypothesis), *a la* the MDAC approach. The 2D grids represent log Pn/Lg spectral ratios for all combinations of frequencies for the Pn and Lg spectra. The spectra are limited to signal-to-noise ratio (SNR) greater than 2. The grid for the earthquake (upper left in Figure 3) has values near zero and little variability over the usable bandwidth of Pn and Lg, as it should, if properly corrected. Alternatively, the grids for the explosions exhibit large departures from zero and spectral structure due to overshoot and spectral modulations. Plots on the

right side of Figure 3 show the model predictions of the 2D spectral ratios (corrected by the same Brune source terms as used for the corresponding empirical grids) for an earthquake and explosions in granite. Despite the variability using only WMQ, the model results exhibit similar behavior as the corresponding empirical grids.

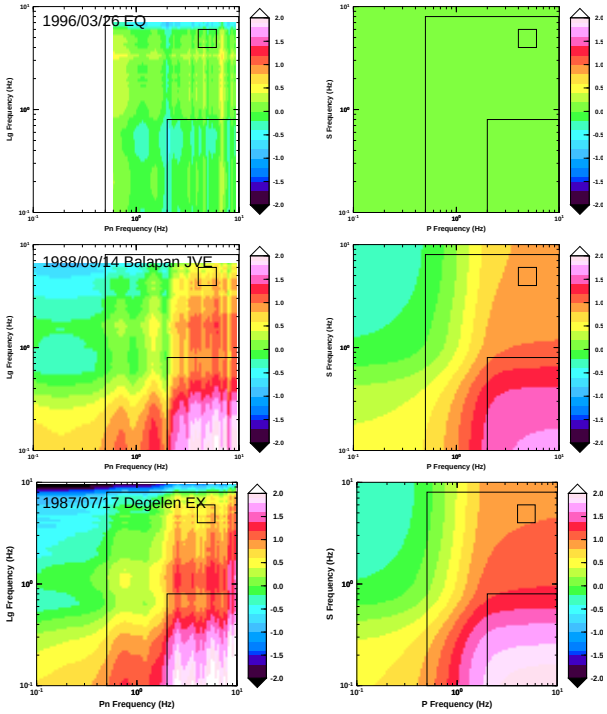

Figure 3. Empirical (left) and model (right) 2D log Pn/Lg spectral ratios for an earthquake (top), the JVE (middle), and a UNE at Degelen (bottom). The grids were computed using only data from WMQ. The three rectangles indicate spectral bands used to measure Pn/Lg ratios for discriminant analyses.

The three rectangles in each plot of Figure 3 are used to measure three types of discriminants. First, the small square represents a typical frequency band of 4–6 Hz for Pn and Lg, often used for a traditional P/S discriminant. Pn/Lg(6–8 Hz) did not improve performance much and there were fewer events with adequate SNR. Second, a cross-spectral ratio is computed as the average log Pn/Lg value for frequencies of Pn and Lg spectra in the 2–10 Hz and 0.1–0.8 Hz bands, respectively. The 2D grids over these frequencies exhibit far more distinction of UNEs and earthquakes than traditional high-frequency P/S. Third, the root mean square (RMS) value of the corrected 2D log Pn/Lg grids are computed over frequencies of 0.5–10 Hz for Pn and 0.1–8 Hz for Lg. This quantifies the misfit of the MDAC model (source, distance, and site terms), under the earthquake hypothesis, to the 2D empirical spectral ratio grid. We refer to these three types of measurements as *traditional*, *cross-spectral*, and *RMS-misfit* Pn/Lg ratios.

Figure 4 shows plots of these three types of log Pn/Lg measurements versus distance to WMQ (left) and mb (right) for earthquakes (circles and black square) and UNEs (stars). The plots show the residual dependence on magnitude and distance after applying the MDAC corrections. Pn/Lg(4–6 Hz) (top plots) provides some separation of explosions and earthquakes, but the overlap and variances limit discrimination performance. Some of the overlap and earthquake variance is due to diverse paths to WMQ. A kriged grid of the earthquake data (Figure 5) varies from –0.34 to 0.32, depending on the path, comparable to the mean separation of the earthquake and explosion populations. The lower four plots of Figure 4 show complete separation of the earthquakes and explosions. The cross-spectral Pn/Lg provides the best separation of the measurements examined. The earthquakes still have large variance, also due to path variations and other effects, but they are not nearly as significant because these new types of spectral ratios vastly increase the mean separation.

Figure 6 shows log Pn/Lg RMS-misfit versus cross-spectral measurements, with the same marker types as in Figure 4. The separation of earthquakes and explosions is remarkable, indicating that their characterization of source differences dominates the effects of path variations. The *RMS-misfit* quantifies how well the MDAC model, assuming a Brune earthquake source term, fits the data. It is generally expected to provide good discrimination, but it can also indicate earthquakes for which the model parameters (e.g., stress drop, Q, geometrical spreading) are inaccurate. Cross-spectral Pn/Lg highlights differences in source characteristics between explosions and earthquakes, based on their different relations of P and S corner frequencies and spectral shapes.

Applying the criteria in Eqs. (1) and (2) (with $N_m = 1$, using only WMQ) to traditional Pn/Lg(4-6 Hz) values, 6 of 28 UNEs (21.4%) and 59 of 72 earthquakes (81.9%) are categorized as *explosion-like* and *earthquake-like*,

respectively. The other events are *undetermined*. Poor performance for the UNEs is mainly due to the large earthquake variance, making it difficult to reject the earthquake hypothesis. Calibration of path effects is one way to reduce this variance and enhance performance.

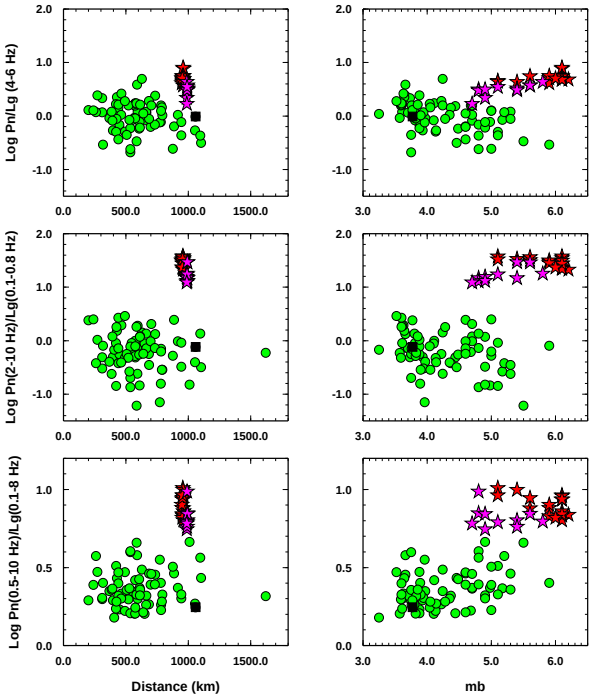

Figure 4. Plots of traditional (top), cross-spectral (middle), and RMS-misfit (bottom) log Pn/Lg values versus distance (left) and mb (right) for earthquakes (circles) and UNEs (stars) at Balapan (red) and Degelen (magenta). The black square in each plot corresponds to the 1996/03/26 earthquake near STS.

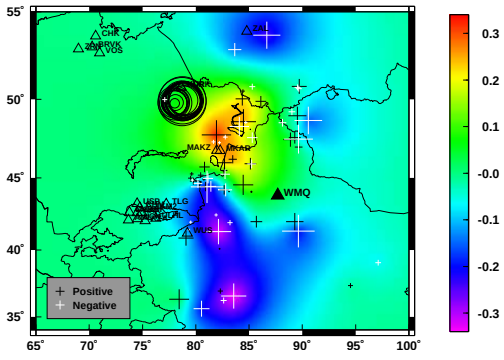

Figure 5. Kriged grid of log[Pn/Lg(4-6 Hz)] for WMQ, based on 72 earthquakes. The markers (size and color) represent residuals to the grid for UNEs (circles) and earthquakes (crosses).

Figure 7 shows results using cross-spectral Pn(2–10 Hz)/Lg(0.1–0.8 Hz) values. All 28 UNEs and 74 earthquakes are categorized properly, even at the 0.0005 significance level. This big improvement is due to the large difference of explosion and earthquake means. There are two more events with adequate SNR for Lg at 0.1–0.8 Hz than 4–6 Hz. For smaller events, even more should have adequate Lg SNR in the lower frequency band. Last, using RMS-misfit Pn(0.5–10 Hz)/Lg(0.1–8 Hz) values, all 28 UNEs and 72 of 74 earthquakes are categorized properly at the 0.005 significance level. The performance is much better than for the traditional high-frequency Pn/Lg and not quite as good as the cross-spectral Pn/Lg.

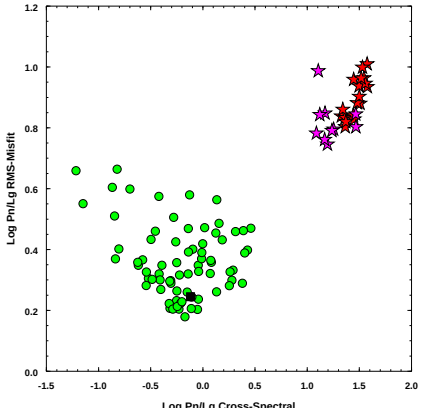

Figure 6. Plot of RMS-misfit versus cross-spectral log Pn/Lg values for earthquakes and STS UNEs.

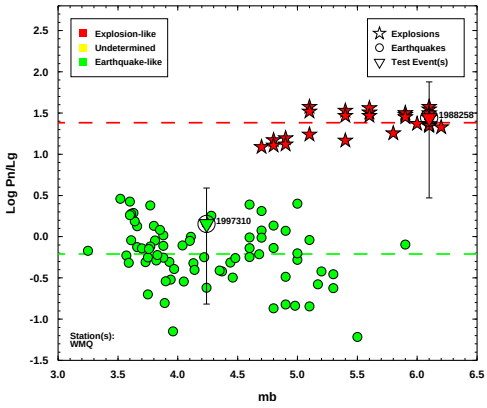

Figure 7. Discrimination results for earthquakes and STS UNEs using cross-spectral Pn/Lg. Dashed lines show population means; 99.5% confidence intervals are shown for the Soviet JVE (1988258) and an earthquake (1997310). All events are categorized properly, even at the 99.95% confidence level.

Lop Nor Test Site

We performed similar analyses for LNTS events; Fisk et al. (2007) show plots like Figures 2 and 3. Figure 8 shows network-averaged Pn/Lg (left) and Pn/Sn (right) versus mb in the same frequency bands defined above. The square in each plot corresponds to the 1999/01/27 earthquake at LNTS. Traditional Pn/Lg and Pn/Sn (top plots) perform better than at STS because the paths for the earthquakes and UNEs are more similar and also due to averaging over many stations. Even so, as for STS, the cross-spectral discriminants (middle plots) exhibit a much better separation of explosions and earthquakes than traditional P/S. The variances are larger for smaller earthquakes because they were generally recorded by fewer stations with adequate SNR. The 1988/09/29 UNE was recorded at regional distance by only WMQ. Its discriminant values are all the highest of these events and tend to inflate the variances for the UNEs. No other LNTS UNEs have WMQ data for comparison. The plots for Pn/Lg and Pn/Sn are fairly similar for a given band, leading to similar discrimination results using either Pn/Lg or Pn/Sn. In the following, we focus on Pn/Sn.

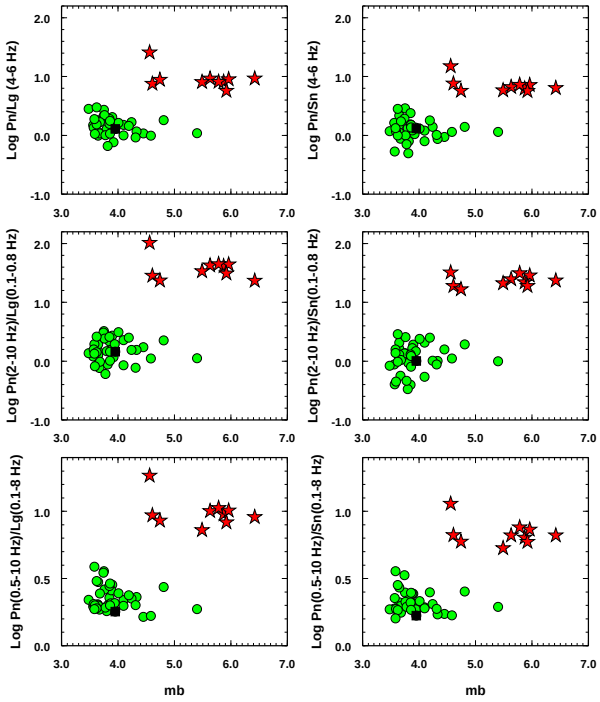

Figure 8. Network-averaged log Pn/Lg (left) and log Pn/Sn (right) measurements versus mb for LNTS UNEs and earthquakes in three combinations of frequency bands, as in Figure 4.

Applying Eqs. (1) and (2) to traditional Pn/Sn(4–6 Hz) values, all 10 UNEs and 41 of 43 earthquakes (95.3%) are categorized properly. Two events are *undetermined*. (N_m ranges from 1 to 19 for the various events.) By most standards, this performance is very good. However, using cross-spectral Pn(2–10 Hz)/Sn(0.1–0.8 Hz) values for the same events, all events are categorized properly even at a very small significance level of 0.00005, a factor of 100 smaller than used for the traditional Pn/Sn. As for STS, this is a vast improvement in discrimination performance. Processing even smaller earthquakes and over a broader area would more clearly demonstrate the benefit, largely due to the increased separation of the earthquake and explosion means for cross-spectral P/S. Using RMS-misfit Pn(0.5-10 Hz)/Sn(0.1-8 Hz) values, all 10 UNEs and 40 of 43 earthquakes are categorized properly at the 0.005 significance level.

Nevada Test Site

We now apply the spectral processing and discrimination methods to NTS. Unlike granite at STS and LNTS, the geology at NTS consists of tuff, rhyolite, and alluvium, with varying degrees of gas porosity (GP), especially above the water table at Yucca Flat. Walter et al. (2004) assembled a dataset for 151 events in the western U.S., including seismograms, origins from several bulletins, and regional phase picks by Ryall (2005). The UNEs range from ML 2.9 to mb 5.9 and include 40 at Yucca Flat, 18 at Pahute Mesa, and 11 at Rainier Mesa since mid 1979 that were recorded digitally by ELK (Elko, NV), KNB (Kanab, UT), LAC (Landers, CA), and/or MNV (Mina, NV). We also used 37 earthquakes at or near NTS, ML 2.6 to mb 5.7. We computed Pn, Pg, and Lg spectra and corrected for magnitude and distance, using MDAC parameters from Walter and Taylor (2002). Fisk (2007) lists the parameters and provides details of the events, including source and geological parameters for the UNEs (from Springer et al., 2002), and comparisons of empirical and model spectra. We used spectra for the 37 earthquakes, corrected for distance and magnitude, to estimate site corrections. We then applied the magnitude, distance, and site corrections to all of the events.

Figure 9 illustrates 2D grids of log Pn/Lg spectral ratios for earthquakes and UNEs. The spectra are limited to

SNR > 2, which is most restrictive on Pn spectra at lower frequencies. The grids for the earthquakes have values closer to zero and less variability than for the explosions, as they should after applying the corrections that include an earthquake source term. The rectangles in each plot of Figure 9 are used to measure various log Pn/Lg spectral ratios: (1) traditional measurements in the 4–6 Hz and 6–8 Hz bands; (2) the average log Pn/Lg value for frequencies of the Pn and Lg spectra in the 1-8 Hz and 4–10 Hz bands, respectively; and (3) the RMS value of the log Pn/Lg grids over the frequencies of 1-8 Hz for Pn and 0.2–10 Hz for Lg. The log Pn/Lg values were computed and averaged over LNN stations with available data. Figure 10 shows the measurements versus magnitude. The upper plots show that Pn/Lg (4–6 Hz) and Pn/Lg(6–8 Hz) provide useful separation of the explosion and earthquake populations. The lower left plot of Figure 10 exhibits complete separation.

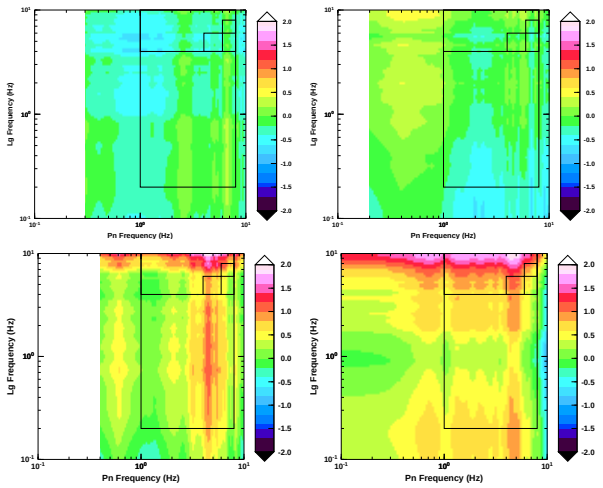

Figure 9. Log Pn/Lg 2D spectral ratios, averaged over stations, for 2 earthquakes (top) and 2 UNEs (bottom). The rectangles depict spectral bands used to measure Pn/Lg ratios for discriminant analyses.

We also considered cross-spectral measurements of log Pn[0.6–8 Hz]/Lg[0.1–1.0 Hz], as we did for LNTS and STS. The performance is good for UNEs in low GP media, but poor for ones above the water table at Yucca Flat, where GP is relatively high (10% to 25%; Springer et al., 2002). Taylor and Denny (1991) describe how an explosion in weak, porous rock has a shock wave that divides into a two-wave system, consisting of an elastic precursor followed by a plastic wave, causing a second effective corner frequency in the source spectrum. They found that Lg spectral amplitudes for such UNEs are especially depleted at higher frequencies. To model Lg spectral ratios for NTS UNEs in media of varying GP, they used the third-order source model (with f^{-3} roll-off and two corner frequencies) of Denny and Goodman (1990). This physical understanding is why we use log Pn[1–8 Hz]/Lg[4–10 Hz], rather than a cross-spectral ratio (with Lg at lower frequencies). As illustrated in the upper larger rectangle in each plot of Figure 9, NTS UNEs consistently exhibit greater differences from earthquakes in this combination of frequency bands.

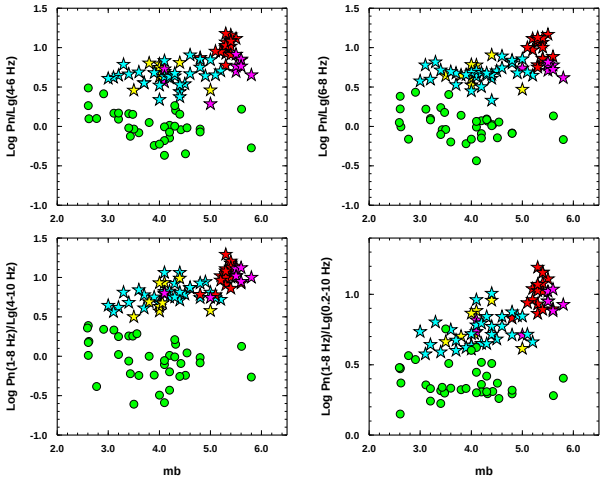

Figure 10. Plots of log Pn/Lg ratios versus mb for NTS UNEs (stars, color-coded as in Figure 11 below), and earthquakes (circles) in four combinations of frequency bands. Average values are shown, except the lower right plot that shows RMS values.

Figure 11 shows a plot of log Pn/Lg RMS-misfit versus log Pn[1–8 Hz]/Lg[4–10 Hz] values. The two types of measurements are highly correlated for the UNEs, indicating by either measure their inconsistency with the earthquake source model. The earthquakes with higher values of the RMS-misfit are typically ones farther from NTS, indicating that the MDAC corrections could be improved to reduce the variance of Pn/Lg data for the earthquake population. The site corrections, estimated from earthquake data that are predominantly at or near NTS, compensate to provide good overall corrections near the test site, but are less accurate away from NTS.

We apply Eqs. (1) and (2) to evaluate the performance of the various Pn/Lg discriminants. Here, N_m ranges from 1 to 4, depending on data availability from various LNN

stations for a given event. The smallest (ML 2.9) UNE, WACO, has insufficient Pn SNR for all cases. For Pn/Lg (4–6 Hz), 66 of 69 (95.7%) UNEs and 28 of 37 (75.7%) earthquakes are categorized properly. Three earthquakes do not have adequate Pn SNR. The other two UNEs and 6 earthquakes are *undetermined*. For Pn/Lg(6-8 Hz), 66 of 69 (95.7%) UNEs and 31 of 37 (83.8%) earthquakes are categorized properly. Of the other two UNEs, one is *undetermined* and one (VILLITA) is mis-categorized as *earthquake-like*. One earthquake does not have adequate SNR and five are *undetermined*. Thus, the performance is somewhat better for 6-8 Hz than 4–6 Hz, except for mis-categorizing VILLITA. It is not mis-categorized if the significance level is reduced to 0.001, but then three UNEs and 10 earthquakes are *undetermined*.

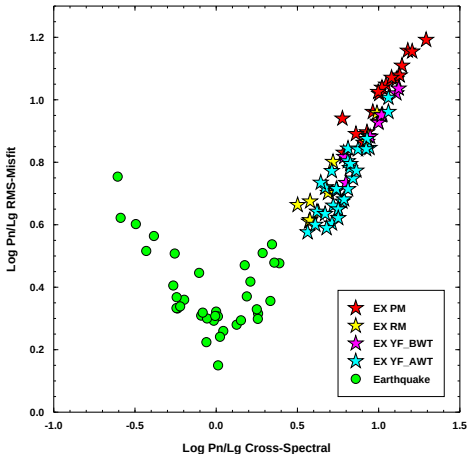

Figure 11. RMS-misfit versus cross-spectral log Pn/Lg values for the NTS UNEs and earthquakes. The stars are color-coded for explosions at Pahute Mesa (PM), Rainier Mesa (RM), and below and above the water table at Yucca Flat (YF_BWT and YF_AWT).

Using log Pn(1-8 Hz)/Lg(4–10 Hz), 68 of 69 UNEs (98.6%; all but WACO) and 34 of 37 earthquakes (91.9%) are categorized properly. The other earthquakes are *undetermined*. All three are relatively small, causing their Pn measurements to be biased high by noise, and they have measurements at only one station, resulting in larger uncertainties. Note that these three earthquakes were also *undetermined* or had insufficient data for the traditional 4–6 Hz and 6–8 Hz bands. The variance of log Pn(1-8 Hz)/Lg(4–10 Hz) values for the earthquake population is somewhat larger than for log Pn/Lg(4-6 Hz). However, the greater separation of earthquake and explosion means improves discrimination performance.

Using the RMS values of log Pn(1-8 Hz)/Lg(0.2–10 Hz), 66 of 69 explosions (95.7%) and 25 of 37 earthquakes (67.6%) are categorized properly. The other events are *undetermined*. Figure 11 shows large RMS values for some earthquakes (thus, they are *undetermined*) due to inconsistencies with the model, even though their average Pn/Lg values are very different from those of explosions. Thus, the RMS measurement is a useful indicator of model inconsistencies, which can be due to source type or various MDAC parameters.

Last, Figure 12 shows observed (cf. Walter et al., 2007) and model Pg and Lg spectra (left) and spectral ratios (right) for the 2006/10/09 UNE in North Korea. Noise effects seem to bias the Pg spectrum at low frequencies. This preliminary comparison suggests that our spectral analyses and modeling will perform quite well here, as at other test sites. Note that the model results, using MM71 for P waves and with shifted corner frequency for S waves (cf. Fisk, 2006, 2007), compare even better for Lg than Pg, similar to findings by Fisk (2007) for NTS.

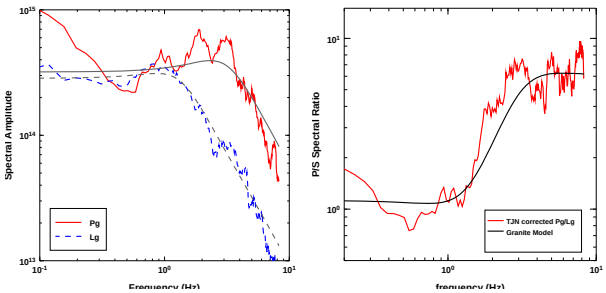

Figure 12. Corrected Pg and Lg spectra (left) and Pg/Lg spectral ratio (right) computed from the TJN recording of the UNE in North Korea on 2006/10/09. Also shown are corresponding model calculations.

CONCLUSIONS AND RECOMMENDATIONS

The MDAC procedure (Taylor and Hartse, 1998; Taylor et al., 2002; Walter and Taylor, 2002), and recent advances by Fisk (2006, 2007) in modeling regional P and S wave spectra for explosions and earthquakes motivated the investigation of 2D grids of P/S spectral

ratios, as a function of all combinations of frequencies for P and S spectra, as a visual technique to assess better discriminants and to facilitate more replete comparisons to model calculations. The 2D P/S grids (shown above) illustrate some key features that are generally observed for a wide range of explosions and earthquakes, also at the test sites in India (Fisk et al., 2007) and North Korea. First, the Pn/Lg and Pn/Sn grids exhibit striking differences between earthquakes and explosions. Second, at hard-rock test sites the differences are most prominent for high frequency Pn and lower frequencies of Lg and Sn. This discriminant utilizes Pn and S-wave spectral content at frequencies mainly above or below the respective explosion P and S corner frequencies. Taylor et al. (2002) advocated cross-spectral P/S ratios. Now there is a model-based interpretation to substantiate their use and visual evidence to guide a more optimal choice of frequencies. Third, comparisons of model calculations to the empirical grids provide compelling evidence, beyond purely statistical metrics, confirming the physical basis of event identification results. The comparisons of the empirical and model grids (e.g., Figure 3) are compelling, not only in how they distinguish earthquakes and explosions, but also the unique signatures within the grids, including patterns and modulations. More detailed analysis of this spectral structure may perhaps be used to further enhance discrimination.

Using Pn/Lg(4–6 Hz) as a baseline case, 59 of 72 earthquakes and only 6 of 28 STS explosions were categorized properly. The other events were *undetermined*. The poor performance to confidently categorize explosions is mainly due to the larger variance of the earthquake population and the overlap of the explosion and earthquake populations when considering events over a wide range of locations. This observation, which is certainly not new, has motivated efforts to calibrate path effects by kriging, tomography, or other methods. Kriging, for example, has been shown to improve discrimination performance substantially. Using the cross-spectral Pn(2–10 Hz)/Lg(0.1–0.8 Hz) measure, all 28 STS UNEs and 74 earthquakes are categorized properly, even at 0.0005 significance (99.95% confidence). Its characterization of source differences dominates the variability from path effects. Further improvements could be obtained by kriging cross-spectral ratios to treat path effects, but this does not seem necessary. This is encouraging because efforts to calibrate path effects for application of P/S ratios to broad areas has been somewhat daunting. In addition to the improved performance, it is expected that many more events will have adequate SNR for Lg in the 0.1-0.8 Hz band than 4–6 Hz, increasing applicability of the cross-spectral discriminant. The benefit is marginal for the datasets used here because the earthquakes (mostly larger than mb 3.6) were originally selected under a previous study to calibrate a traditional Pn/Lg discriminant. Further work is needed to quantify this for smaller events.

The 2D grids and cross-spectral P/S measurements also improve discrimination performance over traditional bands at LNTS. In this case, the earthquakes were localized closer to the test site, and the events were typically recorded by numerous stations. In this case, all of the explosions and earthquakes were categorized properly even at the 0.00005 significance level. The performance is expected to degrade for earthquakes that are smaller, less well recorded, and/or farther from the test site. Nevertheless, this study illustrates the very significant improvement in performance that can be obtained over traditional P/S discriminants.

We also examined the performance of various measurements of 2D log Pn/Lg grids for NTS explosions and nearby earthquakes. The performance of analogous Pg/Lg measurements was not as good as for Pn/Lg, consistent with findings by Walter et al. (1995) and Fisk (2007). As for STS and LNTS, using a traditional Pn/Lg(4–6 Hz) spectral ratio as a baseline case, 95.7% of the explosions and 75.7% of the earthquakes were categorized properly at the 0.005 significance level. Using Pn(1-8 Hz)/Lg(4-10 Hz) values, 98.6% of the explosions and 89.2% of the earthquakes were categorized properly. One UNE (WACO) and three earthquakes could not be categorized, but neither could they be categorized using traditional Pn/Lg measurements. This is a noticeable improvement in performance over the baseline case, although not to the degree at STS for the following reasons. First, the performance of Pn/Lg(4–6 Hz) for NTS events is not as poor as for the STS case because the earthquakes are near NTS, so effects of path variability are much less. Second, there are up to four stations to average over for NTS events. Third, because of geophysical effects of porous rock on Lg from explosions, it was beneficial to use Lg spectral content at higher frequencies

(e.g., 4–10 Hz), especially for explosions above the water table at Yucca Flat. Despite the benefit, this range of frequencies is more similar to traditional high-frequency Pn/Lg. Note that discrimination performance is worse for explosions in media with higher gas porosity and cross-spectral Pn/Lg ratios seem to discriminate poorly for such events. These observations are consistent with the analysis and modeling results for STS and NTS by Taylor and Denny (1991).

Figure 11 suggests that the magnitude and/or distance corrections could be improved to reduce the variance of Pn/Lg for the earthquakes near NTS. In fact, one of the most useful aspects of the RMS-misfit measurements is to assess how well the MDAC model is fitting the spectra over a broad range of frequencies. Further improvements may also be obtained by combining the various spectral ratios in a multivariate test, as suggested by Figure 6. Valid treatment requires adapting the criteria to treat chi-square statistics. Further assessment of the methods is needed for additional and broader regional data.

REFERENCES

Brune, J. N. (1970). Tectonic stress and the spectra of seismic shear waves from earthquakes, *J. Geophys. Res.* 75: 4997–5009.

Denny, M. D. and D. M. Goodman (1990). A case study of the seismic source function: Salmon and Sterling reevaluated, *J. Geophys. Res.* 95: 19,705–19,723.

Fisk, M. D. (2007). Corner frequency scaling of regional seismic phases for underground nuclear explosions at the Nevada Test Site, *Bull. Seism. Soc. Am*. 97: 977–988.

Fisk, M. D. (2006). Source spectral modeling of regional P/S discriminants at nuclear test sites in China and the Former Soviet Union, *Bull. Seism. Soc. Am*. 96: 2348–2367.

Fisk, M. D., S. R. Taylor, H. J. Patton, and W. R. Walter (2007). Next-generation MDAC discrimination procedure using multi-dimensional spectral analyses, in *Proceedings of the 29th Monitoring Research Review: Ground-Based Nuclear Explosion Monitoring Technologies*, LA-UR-07-5613, Vol. 1, pp. 551–560.

Mueller, C. S. and J. R. Murphy (1971). Seismic characteristics of underground nuclear detonations Part I: seismic spectrum scaling, *Bull. Seism. Soc. Am.* 61: 1675–1692.

Ryall, F. (2005). Analysis Summary of an Assembled Western U.S. Dataset, *Lawrence Livermore National Laboratory report, UCRL-TR-210751*.

Springer, D. L., G. A. Pawloski, J. L. Ricca, R. F. Rohrer, and D. K. Smith (2002). Seismic source summary for all U.S. below-surface nuclear explosions, *Bull. Seism. Soc. Am.* 92: 1806–1840.

Taylor, S. R. and M. D. Denny (1991). An analysis of spectral differences between Nevada Test Site and Shagan River nuclear explosions, *J. Geophys. Res.* 96: 6237–6245.

Taylor, S. R. and H. E. Hartse (1998). A procedure for estimation of source and propagation amplitude corrections for regional seismic discriminants, *J. Geophys. Res,* 103: 2781–2789.

Taylor, S. R., A. A. Velasco, H. E. Hartse, W. S. Phillips, W. R. Walter, and A. J. Rodgers (2002). Amplitude corrections for regional seismic discriminants, *Pure Appl. Geophys.* 159: 623–650.

Walter, W. R., E. Matzel, M. E. Pasyanos, D. B. Harris, R. Gok, and S. R. Ford (2007). Empirical observations of earthquake-explosion discrimination using P/S ratios and implications for the sources of explosion S-waves, in *Proceedings of the 29th Monitoring Research Review: Ground-Based Nuclear Explosion Monitoring Technologies*, LA-UR-07-5613, Vol. 1, pp. 684–693.

Walter, W. R., K. M. Mayeda, and H. J. Patton (1995). Phase and spectral ratio discrimination between NTS earthquakes and explosions. Part I: Empirical observations, *Bull. Seism. Soc. Am.* 85: 1050–1067.

Walter, W. R., K. D. Smith, J. L. O'Boyle, T. F. Hauk, F. Ryall, S. D. Ruppert, S. C. Myers, R. Abbot, and D. A. Dodge (2004). An Assembled Western United States Dataset for Regional Seismic Analysis, *Lawrence Livermore National Laboratory report, UCRL-TR-206630*.

Walter, W. R. and S. R. Taylor (2002). A Revised Magnitude and Distance Amplitude Correction (MDAC2) Procedure for Regional Seismic Discriminants: Theory and Testing at NTS, *Lawrence Livermore National Laboratory report, UCRL-ID-146882, LA-UR-02-1008*.